rotational motions spanning about 30° and some occasional larger turns. Phe 30 and Phe 66 both have increased mobility in water compared to in vacuo, and DD time constants are 374 ps for Phe 30 and 397 ps for Phe 66 in the VAC simulation and 20 and 42 ps, respectively, in the AQ simulation. Similar results are obtained for several other internal phenylalanine residues as well, which shows that the presence of water does indeed influence the dynamics not only of external parts of the protein but also of the interior.

Conclusion

The protein structure deviates from its crystal form in all three simulations. This is, of course, a consequence of the potential, but whether it is merely an artifact or a representation of the real conformation remains to be shown. It is certain, though, that the parvalbumin molecule has to be more or less flexible in order to function. Simulation confirms this picture of a fairly flexible molecule.

Water is paramount, and its presence affects the dynamics and structure of the entire protein. Large effects on dynamics are found not only at the surface but also in the interior. The protein structure in aqueous solution more resembles the crystal forms than do the in vacuo ones, as manifested by surface side chains and backbone dihedral angles.

Ligandation of the calcium ions is slightly different for the two binding sites in the crystal form, but not so in the simulations. Exchanges of water ligands do occur, which implies that binding sites are solvent accessible as, indeed, they have to be. Removal of the calcium ions affects local dynamics in all parts of the molecule. The protein is thus capable of fast, global information transfer, a prerequisite of the strong calcium binding cooperativity found from experiment.[70]

The overall translational and rotational diffusions of the protein molecule were each obtained within the correct order of magnitude despite the short duration of the simulation. This is due to the fact that the statistics of these properties are determined by the solvent more than by the solute.

These simulations, especially that in aqueous solution, present a molecule with several interesting properties consistent with the function of parvalbumin. Thus, molecular dynamics simulation is a complement to experiment, even for these very complex systems. For simulation results to be more reliable in detail, though, much validation of inter- and intramolecular potentials as well as more technical aspects remains. In view of the far-reaching advances in the understanding of biomolecular mechanisms then possible, however, these issues deserve great effort.

Acknowledgment is due to Dr. Torbjörn Drakenberg for valuable discussion and encouragement and to the Swedish Natural Science Research Council for generous allocation of computer time.

Registry No. Ca, 7440-70-2.

Supplementary Material Available: Tables of atom types and charges, Lennard-Jones potential parameters, bond length and angle potential parameters, and dihedral angle potential parameters (13 pages). Ordering information is given on any current masthead page.

(70) Teleman, O.; Drakenberg, T.; Forsén, S.; Thulin, E. *Eur. J. Biochem.* **1983**, *134*, 453.

Vibrational Circular Dichroism in Transition-Metal Complexes. 3. Ring Currents and Ring Conformations of Amino Acid Ligands

Teresa B. Freedman,* Daryl A. Young, M. Reza Oboodi, and Laurence A. Nafie*

Contribution from the Department of Chemistry, Syracuse University, Syracuse, New York 13244-1200. *Received August 5, 1986*

Abstract: The enhanced NH and CH stretching vibrational circular dichroism (VCD) spectra of tris(amino acidato)cobalt(III) complexes in acidic aqueous solution and bis(amino acidato)copper(II) complexes in Me_2SO-d_6 solution are interpreted in terms of vibrationally generated ring currents. In the complexes, hydrogen-bonding interactions between an NH bond of one ligand and either an oxygen lone pair (meridional and planar complexes) or a carbonyl π orbital (facial complexes) on an adjacent ligand are identified which restrict the ligand conformations in solution. The VCD spectra are most consistent with the ligand envelope conformations puckered at the metal atom. The large biased NH stretching VCD arises from oscillating current in the ligand and hydrogen-bonded rings generated by the NH vibrational motion.

Vibrational circular dichroism (VCD)[1-5] provides a unique probe for the conformation of chiral molecules in solution, since each vibrational normal mode corresponds to a specific and often localized distortion of the nuclear framework. VCD arises from the generation of nonorthogonal electric and magnetic dipole moments during vibrational excitation. The sign and magnitude of the VCD intensity depend on the manner in which the electrons respond to the nuclear motion. When the electronic motion perfectly follows the nuclear motion, bisignate VCD features may be observed, which are adequately described by the coupled oscillator (CO)[5] or fixed partial charge (FPC)[6] intensity models.

(1) Keiderling, T. A. *Appl. Spectrosc. Rev.* **1981**, *17*, 189.
(2) Nafie, L. A. In *Advances in Infrared and Raman Spectroscopy*; Clark, R. J. M., Hester, R. E., Eds.; Wiley-Heyden: London, 1984; Vol. II, p 49.
(3) Stephens, P. J.; Lowe, M. A. *Annu. Rev. Phys. Chem.* **1985**, *36*, 213.
(4) Freedman, T. B.; Nafie, L. A. In *Tropics in Stereochemistry*; Eliel, E., Wilen, S., Allinger, N., Eds.; Wiley: New York, 1986; Vol. 17, in press.
(5) (a) Holzwarth, G.; Chabay, I. *J. Chem. Phys.* **1972**, *57*, 1632. (b) Sugeta, H.; Marcott, C.; Faulkner, T. R.; Overend, J.; Moscowitz, A. *Chem. Phys. Lett.* **1976**, *40*, 397.
(6) (a) Schellman, J. A. *J. Chem. Phys.* **1973**, *58*, 2282; **1974**, *60*, 343. (b) Deutsche, C. W.; Moscowitz, A. *J. Chem. Phys.* **1968**, *49*, 3257; **1970**, *53*, 2630.

0002-7863/87/1509-1551$01.50/0

In this case, the VCD spectra will be locally unbiased. VCD intensity which is monosignate, or biased to one sign in a local vibrational region (e.g., the antisymmetric NH_2 stretching region), has been recently attributed to a previously unrecognized type of electronic motion, the vibrationally generated electronic ring current.[4,7-13] When a closed pathway is present, due to a covalent or hydrogen-bonded ring, nuclear motion either external to or within the ring can initiate electronic current around the ring that occurs at constant electron density and thus does not contribute to the electric dipole transition moment. In many cases these ring currents provide the predominant electronic contributions to the magnetic dipole transition moment and lead to greatly enhanced VCD intensity.

Based on the VCD spectra of numerous types of molecules and rings, empirical rules have been developed for determining the sense of vibrationally generated current for a given phase of driving nuclear oscillation.[4,10,13] These rules allow one to predict the sign of the VCD of a vibration for various molecular conformations. The observed spectra can thus be correlated with specific solution geometries. Detailed vibrational analyses are usually not required, particularly for localized hydrogen stretching motions.

We have previously found striking examples of ring current enhanced VCD for transition-metal complexes. In the first example,[9] coordination of alanine to a metal was found to increase the VCD bias due to the methine stretch by a factor of 2 or 3, which was attributed to an increased ring current contribution from the ligand ring compared to the CO···HN hydrogen-bonded ring in free alanine at neutral pH. In a study of the VCD of $Co(acac)_2$(L-ala) diastereomers,[11] large enhancement of the NH stretching VCD in the Δ configuration, but not the Λ configuration, was attributed to current generated in a hydrogen-bonded ring joining the L-alanine and an acac ligand, which does not form in the Λ diastereomer. In the previous paper in this series, the enhanced VCD in ethylenediamine complexes[13] was interpreted in terms of currents generated around the ligand rings and around rings formed by halide ion bridges between pairs of ligand NH groups. In all these previous cases, the ring current interpretation provided new, detailed information both on ligand conformation and on intramolecular associations.

The present study concerns bis and tris complexes of α-amino acids.[14,15] The NH and CH stretching VCD spectra of these complexes are interpreted in terms of the ring current mechanism by using the previously established empirical rules. The signs of the predominant VCD features are consistent with solution conformations which maximize intramolecular hydrogen-bonding interactions.

Experimental Section

Tris(glycinato)cobalt(III), $Co(gly)_3$, was prepared[16] by reacting glycine with cobalt(III) hydroxide.[17] The meridional and facial isomers were separated on the basis of solubility differences, and the Λ-*mer*-$Co(gly)_3$ enantiomer was obtained by a bacterial resolution method.[18] The tris complexes of Co(III) and either D- or L-alanine were prepared[16] by reacting the amino acid with either cobalt(III) hydroxide[17] or sodium tris(carbonato)cobalt(III).[19] The geometrical isomers were readily separated due to solubility differences, and the Δ and Λ diastereomers of *mer*- or *fac*-Co(L-ala)$_3$ and *mer*- or *fac*-Co(D-ala)$_3$ were separated by fractional crystallization and liquid chromatography.[9,20,21] The bis Cu(II) complexes Cu(L-pro)$_2$, Cu(D-pro)$_2$, Cu(L-thr)$_2$, and Cu(D-thr)$_2$ were prepared by addition of $Cu(OH)_2$ to solutions of the amino acid.[22] The unreacted $Cu(OH)_2$ was removed by filtration. The identity of each complex was confirmed by visible absorption, electronic circular dichroism, and infrared spectra.

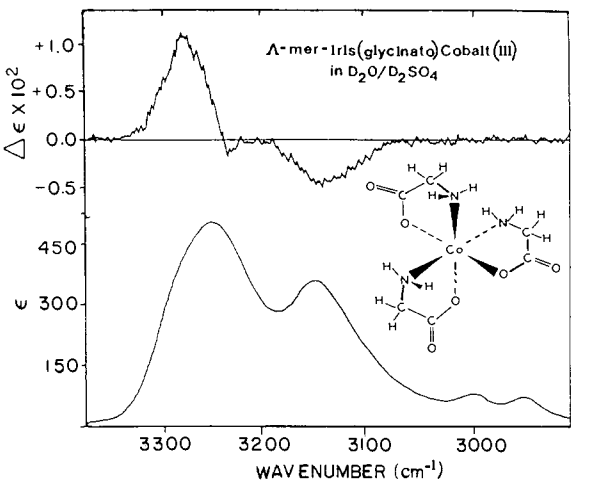

Figure 1. Absorbance and VCD spectra of 0.24 M Λ-*mer*-$Co(gly)_3$ in 9 M D_2SO_4. The path length was 50 μm.

The tris(α-amino acidato)cobalt(III) complexes were dissolved in 9 M D_2SO_4 (99% D, Stohler Isotope Chemicals) or 6 M DCl (99% D, Stohler Isotope Chemicals) which prevented deuterium exchange of the amino groups. Spectra of these samples were obtained with a demountable cell equipped with Infrasil windows and Teflon gasket, spacer, and filling ports. The copper complexes with proline or threonine were dissolved in freshly opened Me_2SO-d_6 (99.5% D, Stohler Isotope Chemicals), and a variable path length cell with CaF_2 windows was used to obtain the spectra.

The VCD spectra in the NH and CH stretching regions were measured at 12-cm^{-1} resolution on a dispersive VCD spectrometer constructed at Syracuse University.[23] Absorption spectra (4-cm^{-1} resolution) were recorded on a Nicolet 7199 FTIR spectrometer. The VCD base lines were obtained by comparing the VCD spectra of the corresponding D and L enantiomers. Since only Λ-*mer*-$Co(gly)_3$ was obtained by the bacterial resolution method, racemic $Co(gly)_3$ was used to obtain the VCD base line of this species.

Results

Bidentate chelation by an amino acid results in tris(amino acidato)cobalt(III) complexes which are either meridional, with identical chelating groups on an edge of an octahedron, or facial, with identical chelating groups on a face of an octahedron. With glycine, only Λ-*mer*-$Co(gly)_3$ was isolated in optically pure form. The VCD and absorption spectra in the 3400–2900-cm^{-1} region for this complex in 9 M D_2SO_4 are presented in Figure 1. The frequencies and assignments are included in Table I. The stretches of the three amino groups give rise to a broad antisymmetric NH_2 stretching absorption band at 3251 cm^{-1} with corresponding positive VCD at 3290 cm^{-1} and a broad symmetric NH_2 stretching absorption band with negative VCD at 3147 cm^{-1}. No VCD is observed in the CH stretching region associated with the antisymmetric and symmetric methylene stretches at 3002 and 2955 cm^{-1}.

All the possible geometric and configurational isomers of the

(7) Nafie, L. A.; Freedman, T. B. *J. Phys. Chem.* **1986**, *90*, 763.
(8) Nafie, L. A.; Oboodi, M. R.; Freedman, T. B. *J. Am. Chem. Soc.* **1983**, *105*, 7449.
(9) Oboodi, M. R.; Lal, B. B.; Young, D. A.; Freedman, T. B.; Nafie, L. A. *J. Am. Chem. Soc.* **1985**, *107*, 1547.
(10) Freedman, T. B.; Balukjian, G. A.; Nafie, L. A. *J. Am. Chem. Soc.* **1985**, *107*, 6213.
(11) Young, D. A.; Lipp, E. D.; Nafie, L. A. *J. Am. Chem. Soc.* **1985**, *107*, 6205.
(12) Paterlini, M. G.; Freedman, T. B.; Nafie, L. A. *J. Am. Chem. Soc.* **1986**, *108*, 1389.
(13) Young, D. A.; Freedman, T. B.; Lipp, E. D.; Nafie, L. A., *J. Am. Chem. Soc.* **1986**, *108*, 7255.
(14) Oboodi, M. R. Ph.D. Dissertation, Syracuse University, 1982.
(15) Young, D. A. Ph.D. Dissertation, Syracuse University, 1986.
(16) Mori, M.; Shibata, M.; Kyuno, E.; Kanaya, M. *Bull. Chem. Soc. Jpn.* **1961**, *34*, 1837.
(17) Brauer, G. *Handbook of Preparative Inorganic Chemistry*; Academic: New York, 1965.
(18) Gillard, R. D.; Lyons, J. R.; Thorpe, C. *J. Chem. Soc., Dalton Trans* **1972**, 1584.
(19) Baurer, H. F.; Drinkard, W. C. *Inorg. Synth.* **1966**, *8*, 202.
(20) Dunlop, J. H.; Gillard, R. D. *J. Chem. Soc.* **1965**, 6531.
(21) Denning, R. G.; Piper, T. S. *Inorg. Chem.* **1966**, *5*, 1056.
(22) Yasui, T. *Bull. Chem. Soc. Jpn.* **1965**, *38*, 1746.
(23) (a) Diem, M.; Gotkin, P. J.; Kupfer, J. M.; Nafie, L. A. *J. Am. Chem. Soc.* **1978**, *100*, 5644. (b) Diem, M.; Photos, E.; Khouri, H.; Nafie, L. A. *J. Am. Chem.* **1979**, *101*, 6829. (c) Lal, B. B.; Diem, M.; Polavarapu, P. L.; Oboodi, M.; Freedman, T. B.; Nafie, L. A. *J. Am. Chem. Soc.* **1982**, *104*, 3336.

Table I. Hydrogen Stretching Frequencies, Intensities, and Assignments of the Absorption and VCD Spectra of Tris(amino acidato)cobalt(III) Complexes in Acidic Aqueous Solution

absorption		VCD		
frequency, cm^{-1}	ϵ, $10^3 cm^2$ mol^{-1}	frequency, cm^{-1}	$10^3\Delta\epsilon$, $10^3 cm^2$ mol^{-1}	assignment[a]
		Λ-*mer*-Co(gly)$_3$ in 9 M D_2SO_4		
3251	500	3290	+12	$\nu^a(NH_2)$
		3239	-1.9	
3147	355	3149	-5.3	$\nu^s(NH_2)$
3002	25			$\nu^a(CH_2)$
2955	38			$\nu_s(CH_2)$
		Λ-*mer*-Co(L-ala)$_3$ in 9 M D_2SO_4		
3270(sh)	450	3266	+24	$\nu^a(NH_2)$
3232	548			
		3193	-9.0	
3127	406	3129	-7.0	$\nu^s(NH_2)$
		3060	-1.3	
3003	8	3009	-3.0	$\nu^a(CH_3)$
		2970	-2.5	
2942	42			$\nu^s(CH_3)$
		2930	+2.0	ν(C*H)
		Λ-*mer*-Co(L-ala)$_3$ in 6 M DCl		
3204	390	3222	+10	$\nu^a(NH_2)$
		3132	+1.3	
3106	400	3089	-8.3	$\nu^s(NH_2)$
2994	26	2995	-3.3	$\nu^a(CH_3)$
2945	36			$\nu^s(CH_3)$
2931(sh)	22	2932	+4.0	ν(C*H)
		Δ-*mer*-Co(L-ala)$_3$ in 9 M D_2SO_4		
3268	390			$\nu^a(NH_2)$
3238	536	3250	-8.3	
		3176	-5.8	
3136	395	3094	-6.0	$\nu^s(NH_2$
		3020	-2.0	
2946	42			$\nu^s(CH_2)$
		2930	+2.0	ν(C*H)
		Δ-*mer*-Co(L-ala)$_3$ in 6 M DCl		
3208	327	3215	-3.9	$\nu^a(NH_2)$
3099	385	3057	-2.3	$\nu^s(NH_2)$
2995	36	2995	-1.5	$\nu^a(CH_3)$
2944	33			$\nu^s(CH_3)$
2926(sh)	10	2932	+4.3	ν(C*H)
		Λ-*fac*-Co(L-ala)$_3$ in 9 M D_2SO_4		
3267	408	3248	-40	$\nu^a(NH_2)$
3218	418			
		3176	-18	
3130	436	3105	+42	$\nu^s(NH_2)$
2972	29	2970	+10	
		Λ-*fac*-Co(L-ala)$_3$ in 6 M in DCl		
3220	318	3215	-26	$\nu^a(NH_2)$
3169	327	3154	-22	
3079	436	3052	+30	$\nu^s(NH_2)$
		3024	+24	
2944	27	2954	+11	
		2908(sh)	+3.3	
		Δ-*fac*-Co(L-ala)$_3$ in 9 M D_2SO_4		
3263	436	3276	+38	$\nu^a(NH_2)$
3226	472	3236	+31	
		3175	-17	
3118	372	3109	-40	$\nu^s(NH_2)$
		3037	-8.0	
3012	10			
2944	36	2946	-7.0	
		Δ-*fac*-Co(L-ala)$_3$ in 6 M DCl		
3212	295	3231	+20	$\nu^a(NH_2)$
3173	300	3121	+12	
3086	354	3050	-25	$\nu^s(NH_2)$
2995	36	2986	-12	
		2931	+0.8	

[a] ν^a = antisymmetric stretch, ν^s = symmetric stretch, sh = shoulder.

tris complexes of Co(III) with L-alanine (or D-alanine) were isolated, the meridional forms denoted Λ-α-tris(L-alaninato)cobalt(III) and Δ-α′-tris(L-alaninato)cobalt(III) and the facial isomers Λ-β-tris(L-alaninato)cobalt(III) and Δ-β′-tris(L-alaninato)cobalt(III). The structures and the hydrogen stretching absorption and VCD spectra of these complexes are presented in Figure 2, with the frequencies, intensities, and assignments compiled in Table I.

The spectra of the alaninato complexes are more structured than those of the glycinato complex. For D_2SO_4 solutions, the NH_2 stretching absorptions occur as two main features at ~3230 and 3130 cm^{-1}. The antisymmetric stretching band has a high-frequency shoulder which is more resolved in the facial isomers. In DCl solution, the NH_2 stretching absorption bands broaden and shift to lower frequency, indicative of ion association between the amino groups and chloride ions.[24] Although the VCD spectra are more structured and have features that do not correspond to absorption maxima, it is evident that in both D_2SO_4 and DCl, the VCD associated with either antisymmetric or symmetric NH_2 stretching is almost totally biased to one sign. In the Δ-*fac* and Λ-*mer* complexes, the antisymmetric NH_2 stretching VCD is positive and the symmetric NH_2 stretching VCD is negative, whereas in the Λ-*fac* complex, the antisymmetric NH_2 stretching VCD is negative and the symmetric NH_2 stretching VCD positive. In contrast, negative VCD in both regions is observed for the Δ-*mer* species. The negative feature near 3180 cm^{-1} in D_2SO_4 solutions of all four isomers is anomalous and may be due to a combination band (e.g., $\nu^a(CO_2) + \delta^a(CH_3)$) rather than to an amino stretching motion.

In the CH stretching region of the meridional complexes, weak absorption at 2945 cm^{-1} and positive VCD features at ~2930 cm^{-1} are observed which have the same magnitude for both diastereomers. The VCD band can be associated with the methine stretch, since $C_\alpha H$ stretching gives rise to positive VCD of similar intensity at 2960 cm^{-1} for neutral D_2O solutions of Δ-*mer*-Co(L-ala)$_3$ (with ND_2 groups).[9] In the facial complexes, the methine VCD at 2930 cm^{-1} is obscured by overlapping VCD intensity having the same sign as the NH_2 symmetric stretching VCD. This intensity probably arises from overtone or combination bands in Fermi resonance with the symmetric NH_2 stretch. In the meridional complexes, the NH stretching VCD is 2–4 times weaker than that in the facial complexes and does not interfere with $C_\alpha H$ stretching VCD. Since the facial complexes are not soluble in neutral D_2O, we were unable to obtain CH stretching VCD spectra of the complexes with deuteriated amino groups.

The bis(amino acidato)copper(II) complexes have square-planar coordination which can be either cis or trans. The trans form is more stable in solution.[25] Only the proline and threonine complexes were sufficiently soluble in Me_2SO-d_6 to permit good quality VCD spectra to be obtained. The hydrogen stretching spectra of the two complexes are shown in Figure 3 and Table II. In Cu(L-pro)$_2$ the NH stretches give rise to a single absorption feature at 3199 cm^{-1}, exhibiting negative VCD. The methylene and methine stretches of the L-proline ring produce a complex pattern of absorption and VCD features between 2800 and 3000 cm^{-1}. In Cu(L-thr)$_2$, the antisymmetric and symmetric NH_2 stretches produce intense absorption features at 3270 and 3155 cm^{-1} but only very weak VCD. The assignments of the CH stretching features given in Table II are based on those for the free ligand.[14] The CH stretching absorption and VCD spectra of the two copper complexes in Me_2SO-d_6 are similar to those previously observed for D_2O solutions.[9,14]

Discussion

The VCD corresponding to each type of local NH stretching motion (NH_2 antisymmetric, NH_2 symmetric, or lone NH) in the α-amino acidato transition-metal complexes is either monosignate or heavily biased to one sign with the exception of Cu(L-thr)$_2$,

(24) Bellamy, L. J. *The Infrared Spectra of Complex Molecules*; Chapman and Hall: New York, 1980; Vol. 2, p 241.
(25) Melnik, M. *Coord. Chem. Rev.* **1982**, *47*, 239.

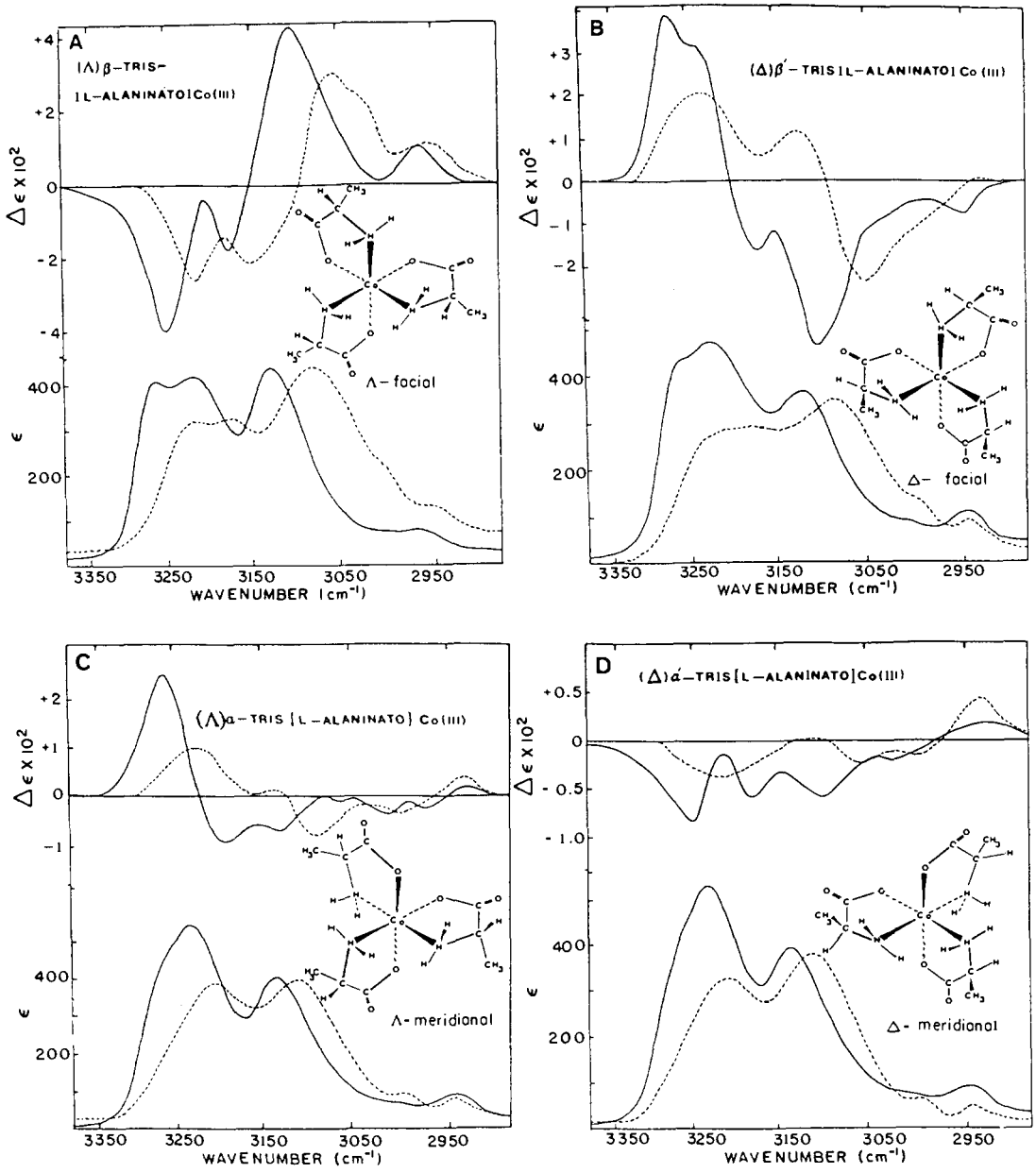

Figure 2. VCD and absorbance spectra of tris(L-alaninato)cobalt(III) complexes in 9 M D_2SO_4 (—) and 6 M DCl (---), 50-μm path length. (A) Λ-*fac*-Co(L-ala)$_3$; 0.17 M in D_2SO_4, 0.13 M in DCl. (B) Δ-*fac*-Co(L-ala)$_3$; 0.39 M in D_2SO_4, 0.34 M in DCl. (C) Λ-*mer*-Co(L-ala)$_3$; 0.22 M in D_2SO_4, 0.23 M in DCl. (D) Δ-*mer*-Co(L-ala)$_3$; 0.44 M in both D_2SO_4 and DCl.

which exhibits only very weak NH stretching VCD. The VCD arising from exciton coupling and frequency splitting due to dipolar interactions among the NH stretches on various ligands in the complex should give rise to conservative VCD couplets in each NH stretching region.[15] Clearly, an additional mechanism that results in monosignate VCD contributions dominates the VCD of these complexes.

Biased NH stretching VCD is also observed in $[Co(en)_3]^{3+}$ salts (en = ethylenediamine) and bis(acetylacetonato)(L-alaninato)-cobalt(III), which have been discussed in the first two publications in this series.[11,13] The enhanced NH stretching VCD in these complexes has been interpreted in terms of large magnetic dipole transition moments arising from vibrationally generated electronic current in rings closed by hydrogen bonding between ligands or current in the ligand ring itself. Similar interpretations can be formulated for the VCD in the amino acid complexes, which lead to information on the solution conformation of the rings.

VCD intensity is proportional to the rotational strength $R = \mathrm{Im}(\boldsymbol{\mu}\cdot\mathbf{m})$ where $\boldsymbol{\mu}$ is the electric dipole transition moment, $\mathbf{m}$ is the magnetic dipole transition moment, and Im denotes the imaginary part. With harmonic oscillator wave functions, the rotational strength for a fundamental transition $0 \rightarrow 1$ for normal mode Q_a with conjugate momentum P_a can be expressed as eq 1[7] for the position form of the electric dipole moment operator.

$$R_{01}{}^{a} = \frac{\hbar}{2}\left(\frac{\partial \mu}{\partial Q_a}\right)_{0,0}\left(\frac{\partial \boldsymbol{m}}{\partial P_a}\right)_{0,0} \qquad (1)$$

Zeroes denote equilibrium values. The sign of R_{01}, and therefore the sign of the VCD intensity, can be predicted if one can determine the directions of the electric dipole moment produced by the nuclear displacements, $(\partial\mu/\partial Q_a)_o$, and the magnetic dipole moment produced by the nuclear momenta, $(\partial \boldsymbol{m}/\partial P_a)_o$.

For localized motions such as NH and CH stretches, the direction of μ for a given phase of a normal mode is readily obtained, since it has been shown from molecular orbital calculations that elongation of a single NH bond results in positive μ directed N $\rightarrow$ H and elongation of a CH bond results in positive μ directed C $\leftarrow$ H.[26] The direction of the ring current contribution to the

(26) Wiberg, K. B.; Wendoloski, J. J. *J. Phys. Chem.* **1984**, *88*, 586.

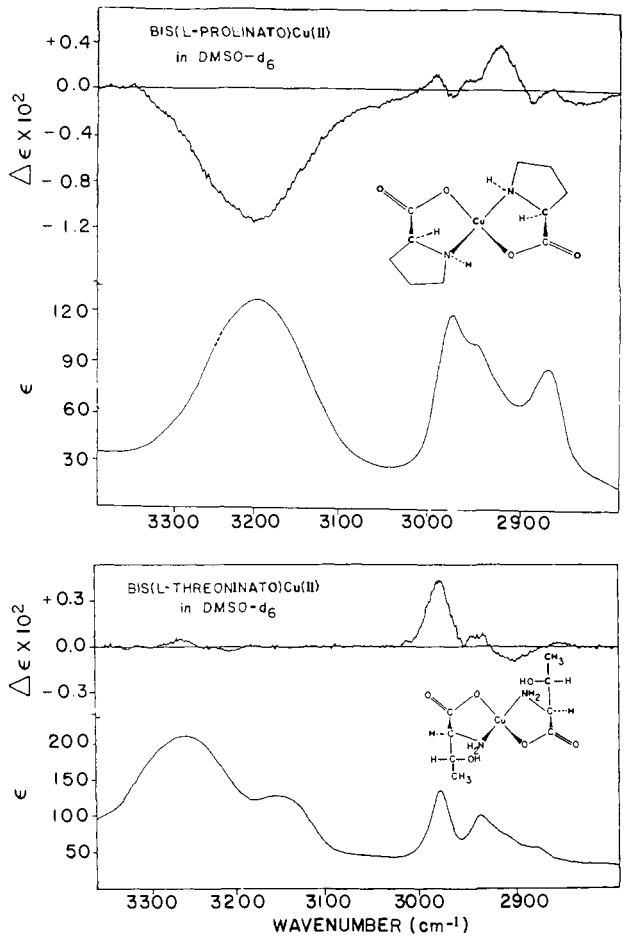

Figure 3. VCD and absorbance spectra of bis(L-amino acidato)copper(II) complexes in Me_2SO. (A) Cu(L-pro)$_2$; 0.298 M, 100-μm path length. (B) Cu(L-thr)$_2$; 0.083 M, 200-μm path length.

magnetic dipole transition moment can be determined from the expression[7]

$$\left(\frac{\partial \boldsymbol{m}}{\partial P_a}\right)_0 = \frac{1}{c}\left(\frac{\partial I}{\partial P_a}\right)_0 \sum_{n\to l} \frac{1}{2}\mathbf{R}_{n,0} \times \mathbf{R}_{l,0} \qquad (2)$$

where $(\partial I/\partial P_a)_o$ is the magnitude of the current around the ring (at constant electron density) generated by the vibrational motion and the summation $n\to l$ is taken around the ring over all pairs (n,l) of adjacent nuclei at equilibrium positions $\mathbf{R}_{n,o}$ and $\mathbf{R}_{l,o}$, in the direction of positive current. For several types of vibrations and rings, the sense of ring current due to a given phase of driving nuclear oscillator can be determined on the basis of empirical rules derived from the VCD spectra of a wide variety of molecules.[4,8-13] Two of these rules[4,10] are pertinent to the NH and CH stretching VCD in amino acid complexes.

Rule 1. When an oscillator attached to a ring contracts, electrons are inserted into the ring such that positive current flows preferentially toward the inducing oscillator along the bonded region having less tightly held electron density. Elongation of the oscillator withdraws electrons from the ring, generating the opposite sense of positive current.

For an NH stretch adjacent to a ring closed by transition-metal coordination, the less tightly held electron density is in the N–M bond, and NH contraction results in positive ring current directed M → N. Furthermore, it has been observed that equatorial hydrogen stretching motion is more effective in generating ring current than axial hydrogen stretching motion, which can be attributed to the larger nuclear momentum component in the ring plane for equatorial compared to axial NH stretch.

Rule 2. When an oscillator involved in a hydrogen-bonding interaction elongates, the hydrogen bond length decreases, strengthening the bond and generating electron flow from the more electron rich of the hydrogen-bonding atoms into the hydrogen-bonded region. For X–H···Y, positive current flows from the hydrogen-bonded region toward Y, the electron-rich substituent, during X–H elongation and away from Y during the X–H contraction.

Table II. Frequencies, Intensities, and Assignments of the Hydrogen Stretching Absorption and VCD Spectra of Bis(amino acidato)copper(II) Complexes in Me_2SO-d_6 Solution

absorption		VCD		
frequency, cm^{-1}	ϵ, $10^3 cm^2\ mol^{-1}$	frequency, cm^{-1}	$10^3\Delta\epsilon$, $10^3 cm^2\ mol^{-1}$	assignment[a]
		Cu(L-pro)$_2$		
3199	128	3196	−12	ν(NH)
		2992	+1.2	
2976	120	2975	−0.5	
		2962	+0.6	$\nu^a(CH_2)$
2950	103	2927	+4.1	ν(C*H)
2880	88	2896	−1.0	$\nu^s(CH_2)$
2826	25	2856	−1.0	
		Cu(L-thr)$_2$		
3270	212	3269	+1.5	$\nu^a(NH_2)$
		3208	−0.5	
3155	125			$\nu^s(NH_2)$
		3005	+0.4	
2975	138	2971	+4.3	$\nu^a(CH_3)$, $\nu(C^*H_\alpha)$
2936	100	2937	0.7	$\nu^s(CH_3)$
2910	70	2898	−0.9	$\nu(C^*H_\beta)$
2880	55	2865	−0.3	

[a] See Table I.

For an NH_2 group with one bond involved in a hydrogen-bonded ring, the symmetric or antisymmetric NH_2 stretches can have an electric dipole transition moment which lies out of the ring plane. Thus ring current enhancement of NH_2 stretching VCD is possible even for a planar hydrogen-bonded ring.

The hydrogen stretching VCD spectra of the α-amino acidato metal complexes included in this study can be interpreted in terms of ring current enhancement governed by rules 1 and 2. Enhancement of NH_2 stretching due to current in the ligand ring, rule 1, requires that the ring be puckered such that one NH bond is in a more axial position and the other more equatorial. The pucker permits net ring current from the two opposing NH motions in the antisymmetric stretch and directs the NH_2 symmetric stretching electric dipole transition moment out of the ring plane. Enhancement due to rule 2 will be greatest for the strongest hydrogen-bonding interaction between ligands, that is, when an NH bond on one ligand is directed toward a lone pair on the coordinated oxygen of an adjacent ligand. The sign of the VCD thus provides information on the sense of ligand ring pucker and the extent and strength of ligand–ligand interaction. The ring current contribution also depends on the area of the ring. Any intramolecular associations which enlarge the ring pathway will increase the VCD arising from current in the ring.

It has been previously calculated that a wide range of amino acid ligand ring conformations correspond to a broad minimum energy region, including both axial and equatorial orientations for the side group.[27] From crystal structure determinations for complexes containing one to three amino acid ligands, a variety of nonplanar ring conformations have been found, including puckered and asymmetric envelope geometries.[28] In crystals, the Co–N–C_α–C′ torsion angle is usually observed to be the largest torsion angle in the ring, resulting in axial and equatorial orientations of the two ligand NH bonds. In solution, it is, therefore, likely that the rings can assume a range of conformations and that the conformation can be influenced by stabilizing ligand–ligand hydrogen-bonding interactions.

For reasons to be given below, for all the hydrogen stretching VCD observed for solution samples of the complexes included in

(27) Gollogly, J. R.; Hawkins, C. J.; Wong, C. L. *Inorg. Nucl. Chem. Lett.* **1970**, *6*, 215.
(28) Pavelcik, F. *J. Coord. Chem.* **1984**, *13*, 299.

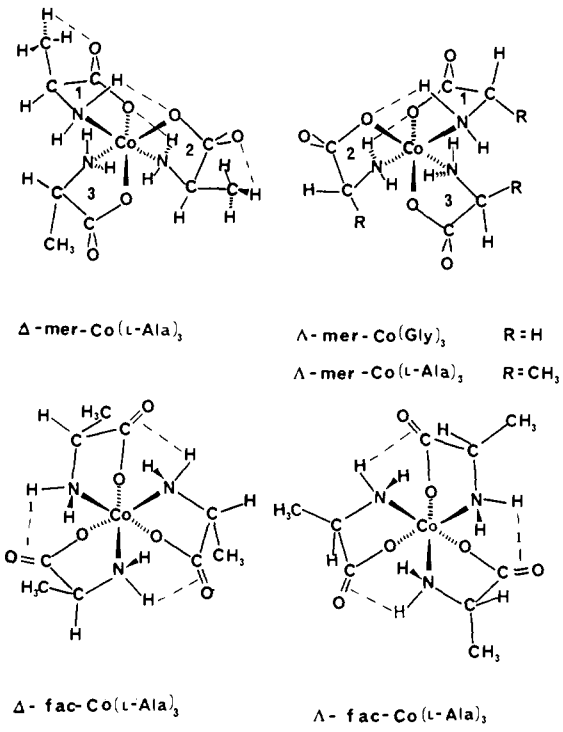

Figure 4. Structures of tris(amino acidato)cobalt(III) complexes showing intramolecular hydrogen-bonding interactions (---) in facial and meridional isomers.

the present study, a consistent interpretation can only be based on the two possible envelope conformations for the ligand ring puckered at the Co apex, **1** and **2**. In this conformation, the C=O

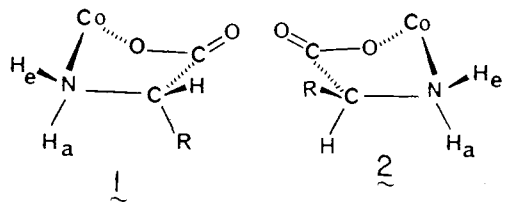

group lies in the plane bisecting the angle between the C_α–H and C_α–R bonds. Evidence supporting this conformation for at least two of the three rings in each meridional complex is presented below. Except in the glycine complexes, some slight additional twist about the C_α–C′ bond may occur to relieve unfavorable steric interactions with the side chain; however, the extent of this twist cannot be determined from the VCD measurements. Construction of molecular models demonstrates that with this ring conformation, the R group is reasonably unhindered, and favorable intramolecular ligand–ligand hydrogen-bonding interactions are possible. As shown for the tris cobalt complexes in Figure 4, in the facial complexes, hydrogen bonding between the axial NH bond of each ligand and the π orbital of the carbonyl on the adjacent ligand can occur. This type of interaction stabilizes the conformation of the complex having all three rings with conformation **1** in the Λ-*fac* configuration and all three rings with conformation **2** in the Δ-*fac* configuration. In the meridional complexes, ligands 1 and 2 (Figure 4) can mutually interact through NH···O hydrogen bonding involving the axial NH bond on one ligand and a σ lone-pair orbital on the coordinated oxygen of the adjacent ligand. This interaction is possible only when both NH_2 groups are puckered as in conformation **1** for the Δ-*mer* configuration or conformation **2** for the Λ-*mer* configuration. Ligand 3 is not involved in strong hydrogen bonding and will adopt conformations which minimize unfavorable steric interactions. Analysis of the crystal structure of Δ-*mer*-Co(L-ala)$_3$ reported by Herak et al.[29]

(29) Herak, R.; Preslenik, B.; Krstanovic, I. *Acta Crystallogr., Sect. B: Struct. Crystallogr. Cryst. Chem.* **1978**, *B34*, 91.

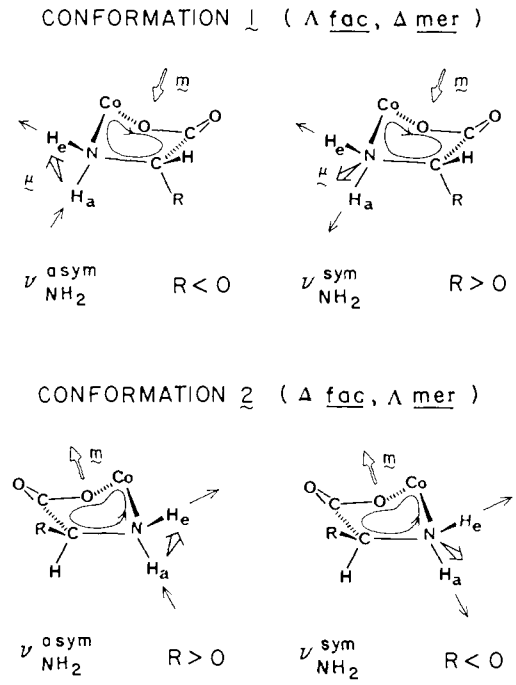

Figure 5. Predicted rotational strengths for NH_2 stretching modes due to vibrationally generated current in the ligand ring. Loop within the ring indicates direction of positive ring current due to equatorial NH_e motion. Open arrows give the positive direction of the electric (μ) and magnetic (m) dipole transition moments.

reveals that two of the ligands do in fact interact through intramolecular N–H_a···O–Co hydrogen bonding in the solid state.

NH Stretching Region. In the facial complexes, it is unlikely that the relatively weak π hydrogen-bonding interaction will provide a significant pathway for vibrationally generated current, and therefore enhanced VCD in the NH_2 stretching modes should arise primarily through current generated about the ligand ring. In Figure 5, the directions of the net electric dipole transition moment and ligand ring current magnetic dipole transition moment are shown for the antisymmetric and symmetric NH_2 stretching modes for the two approximately mirror image ring conformations **1** and **2**. The direction of positive current flow in the ligand ring, depicted by the arrow and loop in each ring, is determined with rule 1 by the motion of the equatorial NH_e bond: elongation of this bond pulls electrons preferentially from the Co–N bond, initiating positive current directed N → Co, while contraction of NH_e pushes electrons preferentially toward the Co atom, initiating the opposite sense of positive current flow.

From the relative orientations of μ and **m** we find that for conformation **1**, negative VCD intensity (proportional to $\mu\cdot\mathbf{m}$) for the antisymmetric NH_2 stretch and positive VCD intensity for the symmetric NH_2 stretch are predicted due to enhancement by current in the ligand ring. For conformation **2**, VCD intensity of the opposite sign is predicted for each corresponding NH_2 stretching region. VCD signals of these same signs are also predicted for conformations which are in addition twisted about the C_α–C′ bond but which retain the same axial and equatorial orientations of the NH bonds as in conformation **1** or **2**.

The signs of the observed NH stretching VCD for the facial complexes, Figure 2a and 2b, agree with the predictions based on a ring conformation stabilized by π hydrogen bonding and vibrationally generated electronic current in the ligand rings: in the Δ-*fac* complex, ring current in the three ligands with conformation **2** produces positive enhanced VCD in the antisymmetric stretching region and negative VCD in the symmetric stretching region. The three rings with the opposite conformation **1** in the Λ-*fac* configuration give rise to enhanced VCD of the opposite sign in each NH stretching region. The equatorial NH bonds in the facial complexes are free to interact with the solvent, and the shift in the NH_2 modes to lower frequency in DCl can thus occur due to NH_e···Cl^- hydrogen bonding.

In the meridional complexes, interpretation of NH stretching VCD spectra, Figures 1 and 2, exclusively in terms of current generated about the ligand ring is not totally satisfactory. The VCD in the Λ-meridional complexes of both L-alanine and glycine follows the pattern predicted for ligand ring current for a majority of the rings constrained in conformation **2**, positive antisymmetric and negative symmetric NH_2 stretching VCD, but the observed VCD for the Δ-*mer*-Co(L-ala)$_3$ complex is negatively biased in both NH_2 stretching regions. As discussed above, in the meridional complexes the intramolecular ligand–ligand hydrogen bonding, through an oxygen σ orbital, is stronger than in the facial complexes. In Δ-Co(acac)$_2$(L-ala), the NH stretching VCD[11] was interpreted in terms of enhancement due to current generated in a similar L-ala···acac hydrogen-bonded ring, **3**. Although in our

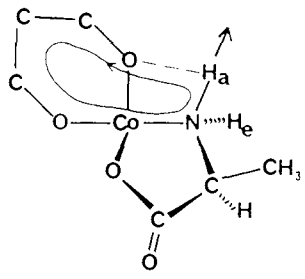

3

earlier report we indicated current only in the Co–O···H–N ring, the remainder of the acac ring is in the same plane as the four-membered hydrogen-bonded ring. Current through the larger area pathway in **3** can readily occur, which will give rise to a larger magnetic dipole transition moment contribution. In this complex, the enhancement due to current in the hydrogen-bonded ring dominates that of the ligand ring in both NH_2 stretching regions. The corresponding hydrogen-bonded rings for the Δ-*mer*- and Λ-*mer*-Co(L-ala)$_3$ complexes, shown in **4** and **5**, respectively, thus

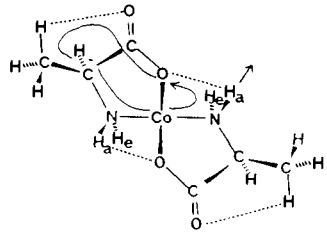

4

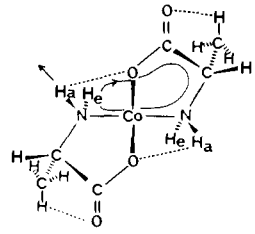

5

provide an additional source for NH stretching VCD enhancement. As shown previously for Δ-Co(acac)$_2$(L-ala),[11] by rule 2, current in the hydrogen-bonded rings for ligands in conformation **1** for Δ-*mer*-Co(L-ala)$_3$ (**4**) results in a positive VCD contribution for antisymmetric NH_2 stretching and a negative contribution for symmetric NH_2 stretching. Contributions of the opposite signs are expected for Λ-*mer*-Co(L-ala)$_3$ (**5**), with ligand rings in conformation **2**. These contributions, due to current in the hydrogen-bonded rings generated by axial NH motion, are all opposite in sign to the corresponding contributions from current in the ligand ring produced by equatorial NH stretching.

An additional type of intramolecular interaction is also important in producing enhanced VCD in these complexes. Interaction between CH groups and π orbitals and lone pairs is not commonly considered a significant source of hydrogen bonding, but there is considerable evidence for such interaction.[30-32] In VCD studies, CH···π or CH···O bonding has been postulated to interpret enhanced VCD features.[10] Studies in our laboratory[33] on the pH dependence of the CH stretching VCD of amino acids and dipeptides and comparisons of the CH stretching VCD of (*S*)-glycine-C_α-d_1, L-alanine, and other amino acids in neutral aqueous solution have provided evidence that interaction between a carbonyl (or carboxylate) lone pair and a β–CH bond produces an important pathway for vibrationally generated ring current. This type of interaction, also shown in **4** and **5**, provides an extended path both for current in the ligand ring generated by equatorial NH stretching motion and for current in the hydrogen-bonded ring generated by axial NH stretching motion. In the Δ-*mer*-Co(L-ala)$_3$ complex, **4**, the extended path contributes to the VCD resulting from the hydrogen-bonded ring, since the plane of the NH_2 group is approximately orthogonal to the C_αCH···O=C plane, which allows μ for either NH_2 stretch and **m** due to current in the CH···O ring to be nonorthogonal. However, in the Λ-*mer*-Co(L-ala)$_3$ complex, **5**, the planes of the NH_2 group and C_αCH···O=C ring are approximately parallel, and current in this ring cannot enhance the NH_2 stretching VCD. In Λ-*mer*-Co(gly)$_3$, no β-hydrogens are present, and the extended pathway is not possible.

We can now provide a consistent interpretation of the NH stretching VCD of the three meridional complexes in terms of contributions from current generated in the ligand rings, the NH···OCo hydrogen-bonded rings, and the CH···O=C hydrogen-bonded rings. In both Λ-*mer* complexes, the current in the ligand ring, generated by the equatorial NH stretch, provides the predominant contribution, and the observed VCD spectrum (Figures 1 and 2c) corresponds to that predicted in Figure 5 for conformation **2**. The magnitude of the NH stretching VCD in the L-alanine complex is approximately twice that of the glycine complex, which can be attributed to the extension of the effective area for the alanine ligand ring current due to the C_αCH···O=C interaction. In Δ-*mer*-Co(L-ala)$_3$, the contribution from current in the NH···O pathway generated by axial NH stretching is increased due to the favorable orientation of the C_αCH···O=C ring. As a result, in comparing Figure 2c and 2d we find that the antisymmetric NH_2 stretching VCD in the Δ-*mer* complex is less negative than expected, due to the larger positive contribution from the hydrogen-bonded rings. In the symmetric NH_2 stretching region of Δ-*mer*-Co(L-ala)$_3$, the negative VCD contribution from the hydrogen-bonded rings predominates over the positive ligand ring VCD contribution, giving rise to the observed negative VCD intensity. From the sum of the VCD intensities of the Δ- and Λ-*mer* complexes, the additional intensity arising from the extended C–H···O=C ring can be estimated as $|\Delta\epsilon| \sim 14 \times 10^{-3}\ 10^3\ cm^2\ mol^{-1}$ for both NH stretching regions. The smaller VCD intensity in the Λ-*mer* complex compared to the Δ-*fac* complex of L-alanine may also result from the opposing contribution of the σ hydrogen-bonded ring, although it is also possible that the non-hydrogen-bonded ligand in the Λ-*mer* complex adopts the opposite configuration to the other two ligands.

CH Stretching Region. VCD arising from the CH stretching modes also provides information on ligand conformation. For Δ-*mer*-Co(L-ala)$_3$, the VCD at 2930 cm^{-1} in acid solution is similar in position and magnitude to that at 2950 cm^{-1} in neutral D_2O solution,[9] in which the amino hydrogens have been exchanged for deuterium. This positive VCD band is assigned to the C_αH stretch, which is enhanced due to current generated by the C_αH stretch around the extended ligand and C_αCH···O=C rings. The ring current sense is governed by rule 1.

The observation that the C_αH stretching VCD spectra in the Λ-*mer*- and Δ-*mer*-Co(L-ala)$_3$ complexes in either D_2SO_4 or DCl solution, Figure 2c and 2d, have the same sign and magnitude suggests similar ring conformations in the two configurations and supports the proposed envelope puckered at the Co atom. In these conformations, **1** and **2**, the C_αCH···O=C interactions are identical and the most favorable, and although the directions of the ring current magnetic moments **m** differ, the overlap of **m** with μ for the C_αH stretch is nearly the same for both ring conformations, as shown for the C_αH contraction in **6** and **7**. Other conformations which retain the ligand–ligand hydrogen bonding but which place the largest degree of puckering at the N or C_α apex would result

(30) Taylor, R.; Kennard, O. *J. Am. Chem. Soc.* **1982**, *104*, 5063.
(31) Meot-Ner, M. *Acc. Chem. Res.* **1984**, *17*, 186.
(32) Tayor, R.; Kennard, O. *Acc. Chem. Res.* **1984**, *17*, 320.
(33) (a) Zuk, W. M.; Freedman, T. B.; Nafie, L. A., unpublished results. (b) Zuk, W. M. Ph.D. Dissertation, Syracuse University, 1986.

in different $C_\alpha H$ enhancements in the two meridional configurations.

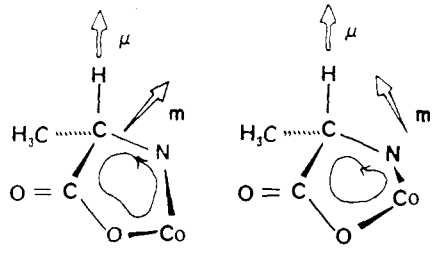

6 7

The absence of observable CH_2 stretching VCD intensity in Λ-*mer*-Co(gly)$_3$ also lends support to conformations **1** and **2**, in which the methylene CH bonds are nearly equivalent. Any ring puckering which leads to nonequivalent equatorial and axial CH bonds would lead to enhanced CH_2 stretching VCD, similar to the mechanism described above for the NH_2 stretches. With equivalent CH bonds, the ring current generated by the opposing motions of the CH bonds in the antisymmetric stretch will cancel, and the electric dipole transition moment for the symmetric CH_2 stretch will be nearly orthogonal to the ring current magnetic dipole transition moment. Ring current enhancement of methylene stretches is observed in sugars[12] and in proline and proline derivatives.[14,34] which have conformations with nonequivalent methylene hydrogen atoms.

In the facial L-alanine complexes, the weaker CH stretching VCD is obscured by contributions from the NH_2 stretching region, which is more intense and extends to a lower frequency compared to the NH_2 stretching VCD spectra of the meridional complexes. Since the amino hydrogens in the facial complexes could not be exchanged in D_2O, due to low solubility at neutral pH, conformational information is not available from the CH stretching modes of the facial complexes.

Bis Copper Complexes. The previous VCD spectra of several bis(amino acidato)copper(II) complexes, obtained in neutral D_2O solution, were restricted to the CH stretching region due to deuterium exchange at the amino groups.[9,14] The copper complexes of L-proline and L-threonine are sufficiently soluble in Me_2SO-d_6 to permit observations of the NH stretching region and the mid-infrared region 1600–1240 cm^{-1}.[15] The bis copper complexes have a planar coordination geometry, and due to the lability of the complexes, the cis and trans forms exist in equilibrium in solution with the trans form more stable.[25] L-Proline chelation results exclusively in the *S* configuration at the nitrogen.[35]

Although enhanced VCD (Figure 3) is observed in the CH stretching region of both the L-proline and L-threonine complexes, significant NH stretching VCD is observed only for the L-proline complex. The differences between the NH stretching VCD spectra of the two complexes can be understood by considering the conformational flexibility of the bis Cu(II) complexes compared to the tris Co(III) complexes. In the tris Co(III) complexes, the mutual intramolecular hydrogen bonding among the ligands can restrict the orientation of the NH_2 groups. In the *trans*-Cu(II) complexes mutual hydrogen bonding can also occur between an equatorial NH bond of one ligand and a lone pair on the coordinated oxygen of the other ligand. However, in threonine there will be equal populations of conformations **8** and **9**, which exist in equilibrium independently for either ligand in the copper complex. For the near mirror image conformations **8** and **9**, the cancellation of VCD signals for corresponding NH_2 modes, which are equal in magnitude but opposite in sign, thus results in practically no net VCD in the NH stretching region of bis Cu(L-thr)$_2$. In any cis complex present, the conformations are not restricted by intramolecular interaction, and no net VCD contribution is likely. The very weak bisignate VCD observed in the antisymmetric stretching regions of Cu(L-thr)$_2$ can arise from incomplete cancellation of the VCD contribution due to slightly different frequencies for the mode in the conformations **8** and **9**.

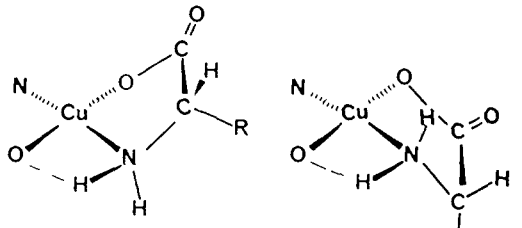

8 9

In *trans*-Cu(L-pro)$_2$, mutual intramolecular hydrogen bonding restricts the ring conformations to structure similar to **10**. The

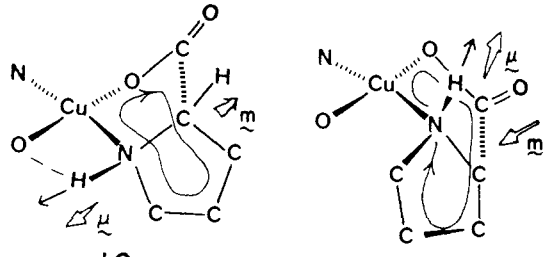

10 11

non-hydrogen-bonded conformer **11** is also possible, and in the cis isomer the conformation is not restricted. With either form **10** or **11**, negative rotational strength is predicted due to current in the ligand and proline rings generated by the lone NH stretch (rule 1), in agreement with the observed spectrum in Figure 3.

Conclusion

We have provided interpretations of the NH and CH stretching VCD spectra for a number of α-amino acidato transition-metal complexes based on the ring current mechanism. The VCD spectra are all consistent with a ligand ring conformation in solution that is puckered at the cobalt apex. The VCD spectra of the free L-alanine ligand at neutral pH have also been interpreted[9,33] on the basis of a similar conformation, which can be derived by replacing the cobalt atom in either **1** or **2** with a hydrogen atom covalently bonded to the nitrogen and hydrogen bonded to the carboxylate oxygen.

Ring current effects appear to completely dominate the VCD spectra of the α-amino acid complexes, as has also been proposed in interpreting the NH and CH stretching VCD spectra of ethylenediamine[13] and β-alanine[36] ligands. No VCD couplets ascribable to coupling among ligand vibrations are observed in the hydrogen stretching regions. The signs and relative intensities of corresponding VCD bands for the series of complexes considered in this study can all be understood on the basis of the ring current mechanism for solution structures stabilized to the maximum extent by intramolecular ligand–ligand hydrogen bonding which can be either NH···O(σ) or NH···O(π) if σ bonding orientations are not possible.

The sense of vibrationally generated ring current follows the previously established empirical rules, rule 1 for the current in the ligand rings, generated by the equatorial NH or methine stretching motion, and rule 2 for the current in the σ hydrogen-bonded rings, generated by the axial NH stretch. The two types of current can generate VCD of opposite signs, and the relative importance of the two effects depends on the strength of the hydrogen bonding and the total area available for electronic current flow, including extended pathways due to CH···O interaction. Thus VCD is found to be sensitive to intramolecular

(34) Freedman, T. B.; Chernovitz, A.; Oboodi, M. R.; Nafie, L. A., unpublished results.

(35) Yasui, T. *Bull. Chem. Soc. Jpn.* **1965**, *38*, 1746. Yasui, T.; Hidaka, J.; Shimura, J. *J. Am. Chem. Soc.* **1965**, *87*, 2762.

(36) Freedman, T. B.; Young, D. A.; Nafie, L. A., unpublished results.

interactions which are not necessarily apparent from other types of physical measurement.

In support of our interpretations, in the crystal of Δ-*mer*-Co(L-ala)$_3$, two short NH···O separations (~2.6 Å) are observed for a pair of ligands, and in addition, the NH_2 and CH_3 orientations in the crystal are quite similar to those deduced from the solution VCD spectra based on competing ring current effects.[29] Although quantitative determination of solution structures is not as yet possible, it is clear that through the ring current mechanism, the VCD spectra for these complexes have provided detailed stereochemical information on the most abundant solution conformations.

Acknowledgment. We acknowledge grants from the National Science Foundation (CHE83-02416) and National Institutes of Health (GM-23567) for financial support of this research.

Communications to the Editor

Resonance Raman Spectra of the [2Fe-2S] Clusters of the Rieske Protein from *Thermus* and Phthalate Dioxygenase from *Pseudomonas*

Debasish Kuila, James A. Fee,*† Jon R. Schoonover, and William H. Woodruff*

Los Alamos National Laboratory
University of California
Los Alamos, New Mexico 87545

Christopher J. Batie and David P. Ballou*

Department of Biological Chemistry
The University of Michigan
Ann Arbor, Michigan 48109-0606

Received August 15, 1986

The iron–sulfur protein of the mitochondrial cytochrome bc_1 complex[1-3] and the photosynthetic cytochrome b_6f complex,[1-3] called the Rieske protein, contains a unique [2Fe–2S] cluster. Its characteristic spectral features have revealed its presence, as well, in the plasma membrane of several bacterial species[1-3] and in certain bacterial oxygenases (cf. ref 4). Recently, the protein from *Thermus thermophilus* was obtained in high purity, found to have M_r = 20000 and contain four Fe, four S^{2-}, and four cysteine residues.[4] Mössbauer and other data[4] gave strong evidence for the presence of two essentially identical [2Fe–2S] clusters, suggesting that each cluster is coordinated to two of the available cysteine residues. Within a cluster, both irons are high spin and each appears to reside in a slightly different coordination environment. An ENDOR study[5] demonstrated the presence of Fe–N bonds, probably histidine imidazoles, but gave no evidence on either the number of nitrogenous ligands or their distribution on the cluster. In this paper we describe a resonance Raman (RR) study of these novel iron–sulfur–nitrogen clusters which provides evidence for an asymmetric distribution of Cys and N ligands on the cluster. The systems examined were *Thermus* Rieske protein (TRP) and phthalate dioxygenase (PDO) from *Pseudomonas cepacia*; we compare the RR spectra of these proteins to that of spinach ferredoxin (SFD).

The [2Fe–2S] clusters of PDO and several other NADH-dependent dioxygenases appear to be structurally similar to those of TRP.[4,6] However, there are differences. For example, the midpoint potentials of the dioxygenases are normally less than −100 mV,[7,8] while the midpoint potentials of the clusters in Rieske

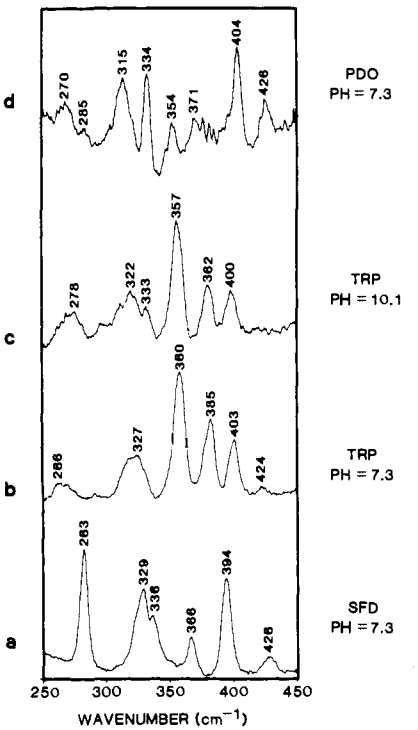

Figure 1. Resonance Raman spectra: (a) Oxidized spinach ferredoxin at pH 7.3 in HEPES [*N*-(2-hydroxyethyl)piperazine-*N*'-2-ethanesulfonic acid]. The spectrum was recorded with 457.9-nm excitation and 135-mW power and is an average of 53 scans. (b) Oxidized Rieske [2Fe–2S] protein from *T. thermophilus* at pH 7.3, HEPES. The spectrum was recorded with 488.0-nm excitation and 85 mW power and is the average of 40 scans. (c) Oxidized Rieske protein from *T. thermophilus* at pH 10.1, CAPS [(3-cyclohexylamino)-1-propanesulfonic acid]. The spectrum was recorded at 488.0-nm excitation and 110-mW power and is the average of 35 scans. (d) Phthalate dioxygenase from *P. cepacia* in HEPES, pH 7.3. The spectrum was recorded with 457.9-nm excitation and 135-mW power and is the average of 67 scans. Resonance Raman spectra of all the samples were recorded using an Ar^+ CW laser with a resolution of 4 cm^{-1} and a scan rate of 1 cm^{-1}/s. Scattered photons were collected by 135° backscattering off the surface of the frozen protein solution (74 K, ~800 mbar) (cf. Czernuszewicz and Johnson, ref 20). The spinach ferredoxin was purified by the method of Petering et al.[21] *T. thermophilus* Rieske protein was isolated by the method of Fee et al.[5] The protein had $A_{460}/A_{280} > 0.22$ before and after the experiment. Phthalate dioxygenase from *P. cepacia* was isolated by the procedure in ref 22. The $A_{280}/A_{460} = 14$ was used to check the purity of the sample before and after the experiment. The samples for resonance Raman experiments were prepared by passing the sample through a Sephadex G-25 column equilibrated with the buffer and concentrating it by slow evaporation under a stream of argon. The A_{460} of all the samples were >1/mm (i.e., >1 mM).

† Address requests for reprints to this author: INC-4, C-345, Los Alamos National Laboratory, Los Alamos, NM 87545.

(1) Malkin, R.; Bearden, A. J. *Biochim. Biophys. Acta* **1978**, *505*, 147-181.
(2) Trumpower, B. L. *Biochim. Biophys. Acta* **1981**, *639*, 129-155.
(3) Hauska, G.; Hurt, E.; Gabellini, N.; Löckan, W. *Biochim. Biophys. Acta* **1983**, *726*, 97-133.
(4) Fee, J. A.; Findling, K. L.; Yoshida, T.; Hille, R.; Tarr, G. E.; Hearshen, D. O.; Dunham, W. R.; Day, E. P.; Kent, T. A.; Münck, E. *J. Biol. Chem.* **1984**, *259*, 124-133.
(5) Cline, J. F.; Hoffman, B. M.; Mims, W. B.; LaHaie, E.; Ballou, D. P.; Fee, J. A. *J. Biol. Chem.* **1985**, *260*, 3251-3254.

0002-7863/87/1509-1559$01.50/0